MOLECULAR IMAGING AND BIOLOGY

Mol Imaging Biol (2013) 15:450–455
DOI: 10.1007/s11307-013-0612-4

Published Online: 30 January 2013

World Molecular Imaging Society

RESEARCH ARTICLE

Usefulness of ^{11}C-Choline Positron Emission Tomography for Genital Chlamydial Infection Assessment in a Balb/c Murine Model

Antonella Marangoni,[1] Cristina Nanni,[2] Carmelo Quarta,[2] Claudio Foschi,[1] Incoronata Russo,[1] Paola Nardini,[1] Antonietta D'Errico,[3] Francesca Rosini,[3] Alice Ferretti,[4] Rita Aldini,[5] Roberto Cevenini,[1] Domenico Rubello[6]

[1]*Microbiology, DIMES Department, S. Orsola Hospital, University of Bologna, Via Massarenti, 9, 40138 Bologna, Italy*
[2]*Department of Nuclear Medicine, Azienda Ospedaliero-Universitaria di Bologna Policlinico S.Orsola-Malpighi, Bologna, Italy*
[3]*DIMES Department, University of Bologna, Bologna, Italy*
[4]*Medical Physics, Santa Maria della Misericordia Hospital, Rovigo, Italy*
[5]*FaBit Department, University of Bologna, Bologna, Italy*
[6]*Department of Nuclear Medicine, Santa Maria della Misericordia Hospital, Via Tre Martiri 140, 45100 Rovigo, Italy*

Abstract

Purpose: The aim of this study is to explore the feasibility of ^{11}C-Choline PET in the assessment of the degree of inflammation in the *Chlamydia muridarum* genital infection model.

Procedures: Forty female Balb/c mice received 2.5 mg of medroxyprogesterone acetate i.m. 9 and 2 days prior to the infection: 21 mice were infected by *C. muridarum* into the vaginal vault, 12 mice were treated with inactivated chlamydiae, and 7 mice were SPG buffer-treated as negative controls. Three healthy control mice were not treated with progesterone. Mice in each category were randomly subdivided in two groups: (1) sacrificed at 5, 10, 15, and 20 days for histological analysis and (2) undergoing ^{11}C-Choline PET at days 5, 10, and 20 post-infection (20 MBq of ^{11}C-Choline, uptake time of 10 min, acquisition through a small-animal PET tomograph for 15 min).

Results: Infected animals showed a significantly higher standardized uptake value than both controls and animals inoculated with heat-inactivated chlamydiae in each PET scan ($P<0.05$). All organs of the infected animals had scores of inflammation ranging between 2 and 3 at day 5, decreasing to 1–2 at day 20.

Conclusions: This preliminary result demonstrated that ^{11}C-Choline PET can highlight a specific proliferation mechanism of inflammatory cells induced by *C. muridarum*, thanks to a very high sensitivity in detecting very small amounts of tracer in inflammatory cells.

Key words: ^{11}C-Choline PET, Genital chlamydial infection, Small-animal PET

Introduction

Sexually transmitted *Chlamydia trachomatis* infection is an important public health concern because of its adverse effects on reproduction [1]. It has become one of the main causes of tubal factor infertility in women due to the ascending infection in the female genital tract and subsequent pelvic inflammatory disease (PID) [2]. Treatment of acute PID and its complications leads to an increase of health care costs [3].

PID presents a broad spectrum of signs and symptoms, ranging from mild to severe presentations. Most of the laparoscopically confirmed cases of acute PID are

Correspondence to: Antonella Marangoni; *e-mail:* antonella.marangoni@unibo.it

characterized by mild-to-moderate infection. Many studies have demonstrated that approximately two thirds of women with post-infection-associated tubal factor infertility have no history of a previous diagnosis or treatment for acute PID [4, 5]. Since the duration of symptoms is the major determinant of subsequent infertility, early diagnosis and treatment are key points for preserving women's fertility. It follows that the effectiveness of antibiotic therapy is dependent upon the lag time between the onset of symptoms and the correct diagnosis [6].

Although the pathologic consequences of *C. trachomatis* infection are now well established, the mechanisms of tissue damage are not completely understood [7]. *C. trachomatis* infects the columnar epithelial cells of the endocervix and upper genital tract of women and, in prepubescent girls, the transitional epithelium of the vagina. The acute infection is characterized by an infiltration of neutrophils; after 10–14 days, as it becomes chronic, the tissue is invaded by macrophages, lymphocytes, plasma cells, and, less frequently, eosinophils. Histopathologic manifestations include a dense stromal inflammation or microabscess, necrosis of the epithelium or ulceration, and well-formed lymphoid follicles of macrophages and transformed lymphocytes in the germinal center [8].

Multiple animal models of chlamydial infection have been used to examine the inflammatory response that occurs in the female genital tract after *in vivo* inoculation [9] because of difficulties in obtaining information from human tissues. The close similarities of the reproductive tracts—for shape and size—between women and primates provide an attractive model for PID. Such similarities cannot be found in other animal models such as sheep, guinea pigs, pigs, and mice. Moreover, primate PID models can employ the use of human serovars of *C. trachomatis* to induce PID, as they are naturally susceptible to infection [10].

On the contrary, the intravaginal inoculation of *C. trachomatis* in small animals, like mice, produces a self-limiting genital infection [9], and such highly efficient clearance of *C. trachomatis* is mediated by IFN-gamma-induced innate effector mechanisms [11]. Since the use of primates is costly and requires adequate facilities and expert personnel, the most widely used genital animal model of *Chlamydia* infection is now the murine infection due to the mouse pathogen *Chlamydia muridarum* [12]. *C. muridarum* is closely genetically related to *C. trachomatis* [13], and the genital mouse female *C. muridarum* infection is similar to the human female infection with *C. trachomatis*: it affords an ascending infection after intravaginal inoculation that leads to salpingitis, endometritis, tubal fibrosis, and stenosis [9, 11], possibly leading to infertility in phenotypically susceptible mice.

Nowadays, one of the most interesting efforts concerning genital tract infections is to develop new diagnostic techniques for the evaluation of inflammation, which are less invasive than traditional procedures [6, 14, 15]. As an example of translational medicine, in a previous work, we evaluated the ability of positron emission tomography (PET) in the genital mouse model of *C. muridarum* infection [16]. We used ^{68}Ga-chloride PET, but we noticed that gallium was not the optimal tracer to image infective and inflammatory processes, because of its non-specific uptake mechanism. Moreover, the chemical synthesis of ^{68}Ga-chloride requires particular attention in order to maintain a low pH (below 5) and to avoid the presence of gallium hydroxide [16].

^{11}C-Choline is a small molecule that, once intravenously injected, is very quickly integrated as a precursor for the biosynthesis of phospholipids, including phosphatidylcholine, which are essential components of all membranes and modulate signaling processes and the apoptosis pathway within cells [17]. ^{11}C-Choline is subject to very late urinary excretion, so the pelvis is free from urinary radioactivity at the time of image acquisition [18]. For this reason, ^{11}C-Choline has been used for imaging gynecologic tumors [19]. Moreover, Wyss et al. demonstrated that choline avidly accumulates in inflammatory infiltrates [20], and Roivainen et al. showed that ^{11}C-Choline can be regarded as a promising tracer for quantitative imaging of proliferative arthritis changes [21]. Their data have been confirmed by several authors, particularly by Matter [22], Laitinen [23], and Kato [24]. The aim of this study was to explore the feasibility of ^{11}C-Choline PET in the assessment of the degree of inflammation in the *C. muridarum* genital infection model.

Materials and Methods

C. muridarum Culture and Purification

C. muridarum Nigg [16] was a kind gift of Dr. G. Grandi (Novartis Vaccines and Diagnostics S.r.l., Siena). Chlamydiae were grown on confluent monolayers of LLC-MK2 cells, in Earle's minimal essential medium with 1 % (*v*/*v*) L-glutamine, 10 % fetal bovine serum, 1 μg/ml cicloheximide, and 5 g/l glucose. Elementary Bodies (EBs) were purified by sucrose-gradient density centrifugation, as previously described [25]. EBs were harvested, centrifuged, and washed twice with phosphate-buffered saline, resuspended in sucrose phospate glutamate (SPG) buffer, and frozen at −70 °C until use.

Animals Used

All experiments were conducted in conformity with the Public Health Service Policy on Humane Care and Use of Laboratory Animals, and they were approved by the Ethical Committee of the University of Bologna (number protocol 14.06.10). The animals used in this study were 43 female

Balb/c mice, 6 weeks old, purchased from Charles River Laboratories Italia (Calco, Italy). The animals were kept at constant night–day cycling and were allowed the usual commercial diet and water *ad libitum*. All the animals but three received 2.5 mg of medroxyprogesterone acetate i.m. 9 and 2 days prior to the infection. The three animals not treated with progesterone were used as healthy controls.

Model of Infection

Twenty-one mice were infected by placing 15 µl of SPG buffer containing 10^6 inclusion-forming units (IFUs) of *C. muridarum* into the vaginal vault [25]. Twelve animals were treated with 15 µl of SPG containing heat-inactivated 10^6 IFUs of *C. muridarum*. As controls of inflammation, seven animals were challenged with 15 µl of SPG.

Experimental Design

The 21 infected animals were randomly allotted into two groups. In group A, nine animals underwent ^{11}C-Choline PET at days 5, 10, and 20 post-infection. In group B, 12 animals were sacrificed at 5, 10, 15, and 20 days for culture and histological analysis (three animals for each time point). The 12 mice treated with inactivated chlamydiae were divided in two groups as well. In group C, four animals underwent ^{11}C-Choline PET at days 5, 10, and 20 post-inoculation. In group D, eight animals were sacrificed at 5, 10, 15, and 20 days for culture and histological analysis (two animals for each time point). Five inflammation control animals plus one healthy mouse underwent ^{11}C-Choline PET at the same days of the infected animals. Similarly, the remaining two control animals were sacrificed for histological analysis, one at 10 days and the other one at 20 days post-inoculation. At the same days, the remaining two healthy mice were sacrificed for performing histological examination.

^{11}C-Choline PET

^{11}C-Choline was synthesized in a modified commercial synthesis module (TRACERlab, GE Healthcare) according to the solid-phase method, as previously described by Pascali et al. [26]. $^{11}CO_2$ was produced in an on-site cyclotron (PETrace, GE Healthcare) and converted into ^{11}CH3I by the conventional LiAlH4/HI reaction. ^{11}CH3I was used for the *N*-methylation of dimethylaminoethanol (60 µl) directly on a solid-phase support (C18 SepPak Light, Waters). A washing step with ethanol and water was performed, and ^{11}C-Choline, retained on a cation-exchange resin (SepPak Accell Plus CM, Waters), was eluted with saline. Then, it was sterilized by a 0.22-µm filter and collected in a final volume of 8 ml. A high-performance liquid chromatography radiodetector equipped with a reversed-phase column was used to evaluate radiochemical purity. Organic solvents' concentration was measured by gas chromatography. The conventional lysosomal acid lipase method (Cambrex Bioscience) was employed to evaluate endotoxin content. Each animal, anesthetized with gas anesthesia (sevofluorane 3–5 % and oxygen 1 l/min), was injected with approximately 20 MBq of ^{11}C-Choline, in a volume of 0.1 ml, via the tail vein by an insulin syringe. The residual dose was measured to verify the effective dose injected. The animal was subsequently placed on the scanner bed in the prone position. The uptake time was 10 min. Images were acquired with a PET tomograph dedicated to small animals (GE, eXplore Vista DR). The total acquisition time was 15 min [16]. One bed position was sufficient to cover the whole body since the axial field of view of the scanner was 4 cm. Once the scan had been completed, the gas anesthesia was interrupted, and the animal was placed in a warm recovery box until complete recovery. ^{11}C-Choline PET images were reconstructed iteratively (OSEM 2D) and read in three planes (axial, sagittal, and coronal). The scan was considered positive if areas of increased choline uptake were present at sites consistent with the site of inflammation. Semi-quantitative analysis was carried out using the parameter standardized uptake value (SUV), calculated as a ratio of tissue radioactivity concentration (e.g. in units kBq/ml) at time *T*, CPET(T), and injected dose (in units MBq) at the time of injection divided by body weight. In detail, the SUV was calculated as follows: SUV at scan time = uptake (kBq/ml)/injected dose (kBq)/animal weight (g). The target region of interest was placed on the pelvis at the level of the cervical–vaginal region.

Isolation of Chlamydiae from Cervical–Vaginal Swabs and Tissue Homogenates

Infection was monitored by culturing cervical–vaginal secretions, collected by swabs, from all the infected animals at 5, 10, 15, and 20 days post-infection [25]. Moreover, three animals out of group B were sacrificed at 5, 10, 15, and 20 days post-

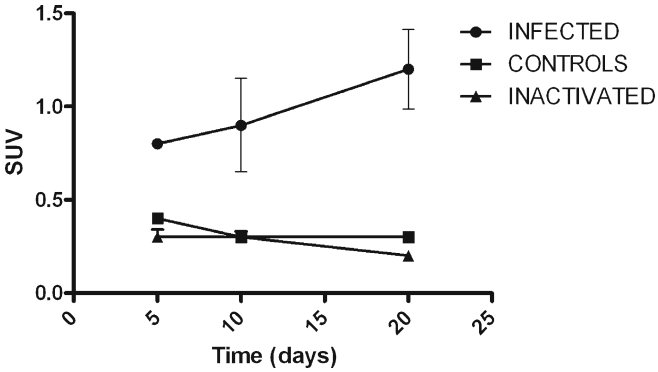

Fig. 1. PET standardized uptake values. SUV in the pelvic region of infected animals, controls, and animals treated with heat-inactivated chlamydiae at 5, 10, and 20 days post-inoculation.

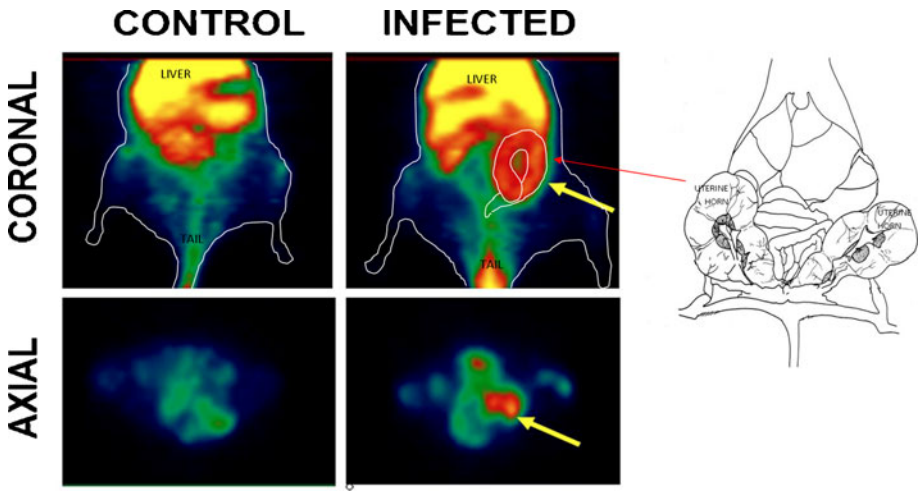

Fig. 2. PET images. Small-animal PET images showing ^{11}C-Choline uptake in the pelvic area (*arrows*) of a representative control and an infected mouse at 10 days post-infection.

chlamydiae inoculation. Genital tracts were divided into the cervical–vaginal region, uterine horns, and oviducts. From each animal, the cervical–vaginal section, the left uterine horn, and the left oviduct were homogenized in a mortar to obtain a 10 % (*w*/*v*) suspension in chlamydial growth medium [27]. LLC-MK2 cells were inoculated, incubated, and fixed as previously reported [25]. Inclusions were visualized by using fluorescein (FITC)-conjugated monoclonal antibody against chlamydia group antigen (Meridian, Cincinnati, OH, USA).

Histology

Right uterine horns and oviducts dissected from the three animals out of group B and two animals out of group D (sacrificed at 5, 10, 15, and 20 days) were stored in formalin and later processed for histological examinations. At 10 and 20 days, two controls and two healthy animals were also sacrificed (one animal for each group at each time), and their genital organs were processed as well.

Four-micrometer-thick sections were cut with Microtome (Leica Microsystems GmbH, Wetzlar, Germany), stained using an automatic staining system (Sakura Finetek USA, Inc., Torrance, CA, USA) with hematoxylin and eosin, and mounted on glass microscope slides. The results were read using a light microscope by investigators blinded to the group of samples being assessed. The uterine horns and oviducts were scored with respect to inflammation using the following criteria: grade 0, no inflammation; grade 1, mild (mild chronic endometritis with no salpinx involvement); grade 2, moderate (moderate acute and chronic infiltrate with focal aggression of the endometrium, tubal, and ovary epithelium, sometimes with lympho-follicular organization); grade 3, severe (large multifocal to coalescing inflammatory neutrophil aggregates, sometimes forming microabscesses with plasma cells and lymphocytes).

Inflammatory aggregates were descriptively characterized as to cell type including lymphocytes, plasma cells, and neutrophils and to the amount of infiltrate in the histological sections.

Statistics

The SUV values of infected animals were compared to the SUV values of animals treated with heat-inactivated chlamydiae and the control of inflammation. Statistical significance was determined by *t* test, and differences were considered significant at $P<0.05$.

Results

PET/CT

The mean SUV max in the pelvic region of infected mice was 0.8±0.4 at the first PET, 0.9±0.3 at the second scan,

Table 1. Score grading of uteri obtained from mice inoculated with live chlamydiae, heat-inactivated chlamydiae, and SPG buffer or from healthy animals, respectively

	Uteri histological grading			
	5 days	10 days	15 days	20 days
Infected animals	2–3	3–3	3–3	1–2
Heat-inactivated chlamydiae-treated animals	0–1	0–1	0–0	0–0
SPG-treated controls	–	0	–	0
Healthy controls	–	0	–	0

Table 2. Score grading of oviducts obtained from mice inoculated with live chlamydiae, heat-inactivated chlamydiae, and SPG buffer or from healthy animals, respectively

	Oviducts' histological grading			
	5 days	10 days	15 days	20 days
Infected animals	2–3	3–3	3–3	1–2
Heat-inactivated chlamydiae-treated animals	0–0	0–0	0–0	0–0
SPG-treated controls	–	0	–	0
Healthy controls	–	0	–	0

and 1.2±0.2 at the third scan. SUV max in controls and inactivated mice was significantly lower in the first scan in comparison to that in infected animals ($P<0.05$). This was true also in the subsequent scans (Figs. 1 and 2).

Histology

The amount of acute and chronic inflammatory cell infiltrate in the endometrium and tubes was assessed. Results obtained are summarized in Table 1 (uterine horns) and Table 2 (oviducts), respectively. At histological examination, no controls showed inflammation in both uteri and oviducts at any time. On the contrary, all the organs from infected animals had scores of inflammation ranging between 2 and 3 at day 5, with a peak at days 10 and 15 when both uteri and oviducts showed an inflammation score of 3, which subsequently decreased at day 20 (range 1–2). No oviducts from animals injected with inactivated bacteria showed inflammation, whereas at days 5 and 10, a mild inflammation (grade 1) was found in one animal out of the three sacrificed at each time point.

Infectivity Assessment

Results of chlamydiae isolation are summarized in Fig. 3. Bacterial burden was significanly decreased at 20 days after infection.

Discussion

Acute PID presents a broad variety of manifestations and symptoms, ranging from evident clinical infection to subclinical infection [4], the latter still being difficult to detect in clinical practice.

The "gold standard" for the diagnosis of subclinical PID is an endometrial biopsy demonstrating acute endometritis [8, 28]. Up to now, studies have tried to identify clinical predictors as well as the presence of subtle symptoms and signs in women with subclinical PID [4, 29]. Unfortunately, no predictors have proved to be clinically useful in the identification of women with subclinical PID.

Moreover, only few patients (up to 20 %) with visually confirmed salpingitis have all the classic symptoms and signs of acute PID. On top of that, no significant differences in the incidence of lower abdominal pain, irregular bleeding, increased discharge, and urinary or gastrointestinal symptoms have been found [5]. Logistical and economical problems make laparoscopy impractical for all patients suspected of acute PID. In addition, laparoscopy cannot diagnose endometritis or cervicitis, and the very early or subtle inflammation of the fallopian tube can be missed.

Imaging techniques have also been suggested as an aid in diagnosing acute PID. As the first-line approach, ultrasonography can be used, whereas magnetic resonance imaging can be seen as an alternative. The extent of PID infection within the abdominal cavity can be assessed with computed tomography (CT) which is also an applied interventional therapy to drain pelvic abscesses [15]. Recently, the CT-confirmative diagnosis of the Fitz-Hugh–Curtis syndrome, a perihepatitis associated to untreated PID, has allowed clinicians to avoid laparoscopy [14, 30].

So far, PET has never been used for the diagnosis of PID, even if this technique has been under evaluation for years for both the diagnosis of gynecological tumors [31] and inflammatory events [32].

2-deoxy-2-[^{18}F]Fluoro-D-glucose is considered the gold standard for inflammation imaging. However, in consideration of its high and physiological excretion via the kidney and longer optimal uptake time (60 min), a very high amount of radioactivity is normally present in the urinary

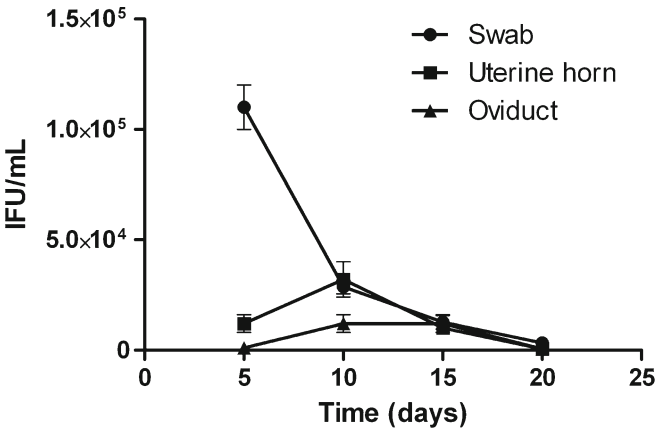

Fig. 3. Results of *C. muridarum* isolation. Isolation of *C. muridarum* from swabs and organ homogenates of the 21 intravaginally infected mice at various days after infection. Infection was monitored by obtaining cervical–vaginal swabs from all the animals on the day of each PET procedure. Moreover, four groups of three animals each were sacrificed at 5, 10, 15, and 20 days after infection, as controls of the infection.

bladder at the moment of image acquisition. This leads to a dramatic decrease of sensitivity for detection of inflammatory areas in the pelvic region. For this reason, in a previous paper of mouse genital infection due to *C. muridarum*, we tried to use ^{68}Ga-chloride as tracer, but we observed that although it seemed to be promising, it was not the optimal radiopharmaceutical to image infective processes because of the inability to differentiate infection from aseptic inflammation [16].

Here, we assessed the diagnostic value of ^{11}C-Choline PET in the diagnosis of inflammatory events due to vaginal *C. muridarum* infection in female mice, since choline is a marker of cellular membrane turnover, which is known to be increased in *Chlamydia*-induced proliferation of inflammatory cells, during infection. The increase in choline uptake in highly proliferative cells such as tumor cells has been related to an up-regulation of choline kinase and increased activity of choline-specific transporters [33]. Regarding inflammation, enhanced choline uptake in activated macrophages has been demonstrated as being caused by increased choline transport, rather than changes in choline kinase [20, 22].

In the present study, infected animals showed a significantly higher SUV than both controls and animals inoculated with heat-inactivated chlamydiae in each PET scan ($P< 0.05$). This preliminary result was in agreement with histological findings proving that ^{11}C-Choline PET is a functional imaging procedure that can highlight a specific proliferation mechanism of inflammatory cells induced by *C. muridarum*, thanks to the very high sensitivity of PET tomographs in detecting very small amounts of accumulated tracer (up to nanograms) into the inflammatory cells.

Although further data are required to confirm our results, this pre-clinical study proposes the use of PET in the diagnosis of PID and opens the way to novel clinical application of PET imaging in the field of inflammation.

Conflict of interest. None

References

1. Beagley KW, Timms P (2000) *Chlamydia trachomatis* infection: incidence, health costs and prospects for vaccine development. J Reprod Immunol 48:47–68
2. Paavonen J, Eggert-Kruse W (1999) *Chlamydia trachomatis*: impact on human reproduction. Hum Reprod Update 5:433–447
3. Rein DB, Kassler WJ, Irwin KL, Rabiee L (2000) Direct medical cost of pelvic inflammatory disease and its sequelae: decreasing but still substantial. Obstet Gynecol 95:397–402
4. Sweet RL, Gibbs RS (2009) Pelvic inflammatory disease. In: Sweet RL, Gibbs RS (eds) Infectious diseases of the female genital tract. Lippincott, Philadelphia, pp 220–244
5. Sweet RL (2012) Pelvic inflammatory disease: current concepts of diagnosis and management. Curr Infect Dis Rep 14(2):194–203
6. Sweet RL (2011) Treatment of acute pelvic inflammatory disease. Infect Dis Obstet Gynecol. doi:10.1155/2011/561909
7. Darville T, Hiltke TJ (2010) Pathogenesis of genital tract disease due to *Chlamydia trachomatis*. J Infect Dis 201(suppl 2):114–125
8. Kiviat NB, Wolner-Hanssen P, Eschenbach DA et al (1990) Endometrial histopathology in patients with culture-proved upper genital tract infection and laparoscopically diagnosed acute salpingitis. Am J Surg Pathol 14:167–175
9. Miyairi I, Ramsey KH, Patton DL (2010) Duration of untreated chlamydial genital infection and factors associated with clearance: review of animal studies. J Infect Dis 201(suppl 2):96–103
10. Bell JD, Bergin IL, Schmidt K et al (2011) Nonhuman primate models used to study pelvic inflammatory disease caused by *Chlamydia trachomatis*. Infect Dis Obstet Gynecol. doi:10.1155/2011/675360
11. Nelson DE, Virok DP, Wood H et al (2005) Chlamydial IFN-gamma immune evasion is linked to host infection tropism. Proc Natl Acad Sci U S A 102:10658–10663
12. Barron AL, White HJ, Rank RG, Soloff BL, Moses EB (1981) A new animal model for the study of *Chlamydia trachomatis* genital infections: infection of mice with the agent of mouse pneumonitis. J Infect Dis 143:63–66
13. Stephens RS, Kalman S, Lammel C et al (1998) Genome sequence of an obligate intracellular pathogen of humans: *Chlamydia trachomatis*. Science 282:754–759
14. Cho HJ, Kim HK, Suh JH et al (2008) Fitz-Hugh–Curtis syndrome: CT findings of three cases. Emerg Radiol 15:43–46
15. Jaiyeoba O, Soper DE (2011) A practical approach to the diagnosis of pelvic inflammatory disease. Infect Dis Obstet Gynecol. doi:10.1155/2011/753037
16. Nanni C, Marangoni A, Quarta C et al (2009) Small animal PET for the evaluation of an animal model of genital infection. Clin Physiol Funct Imaging 29:187–192
17. Zeisel SH (1993) Choline phospholipids: signal transduction and carcinogenesis. FASEB J 7:551–557
18. Nanni C, Fantini L, Nicolini S, Fanti S (2010) Non FDG PET. Clin Radiol 65:536–548
19. Torizuka T, Kanno T, Futatsubashi M et al (2003) Imaging of gynecologic tumors: comparison of $^{(11)}$C-choline PET with $^{(18)}$F-FDG PET. J Nucl Med 44:1051–1056
20. Wyss MT, Weber B, Honer M et al (2004) ^{18}F-choline in experimental soft tissue infection assessed with autoradiography and high-resolution PET. Eur J Nucl Med Mol Imaging 31:312–316
21. Roivainen A, Parkkola R, Yli-Kerttula T et al (2003) Use of positron emission tomography with methyl-11C-choline and 2-18F-fluoro-2-deoxy-D-glucose in comparison with magnetic resonance imaging for the assessment of inflammatory proliferation of synovium. Arthritis Reum 48:3077–3084
22. Matter CM, Wyss MT, Meier P et al (2006) ^{18}F-choline images murine atherosclerotic plaques *ex vivo*. Arterioscler Thromb Vasc Biol 26:584–589
23. Laitinen IE, Luoto P, Någren K et al (2010) Uptake of ^{11}C-choline in mouse atherosclerotic plaques. J Nucl Med 51:798–802
24. Kato K, Schober O, Ikeda M et al (2009) Evaluation and comparison of 11C-choline uptake and calcification in aortic and common carotid arterial walls with combined PET/CT. Eur J Nucl Med Mol Imaging 36:1622–1628
25. Donati M, Sambri V, Comanducci M et al (2003) DNA immunization with pgp3 gene of *Chlamydia trachomatis* inhibits the spread of chlamydial infection from the lower to the upper genital tract in C3H/HeN mice. Vaccine 21:1089–1093
26. Pascali G, D'Antonio L, Bovone P et al (2009) Optimization of automated large scale production of [(18F)]fluoroethylcholine for PET prostate cancer imaging. Nucl Med Biol 36:569–574
27. Marangoni A, Donati M, Cavrini F et al (2006) *Chlamydia pneumoniae* replicates in Kupffer cells in mouse model of liver infection. World J Gastroenterol 12:6453–6457
28. Wiesenfeld HC, Hillier SL, Krohn MA et al (2002) Lower genital tract infection and endometritis: insight into subclinical pelvic inflammatory disease. Obstet Gynecol 100:456–463
29. Wiesenfeld HC, Sweet RL, Ness RB et al (2005) Comparison of acute and subclinical pelvic inflammatory disease. Sex Transm Dis 32:400–405
30. Nishie A, Yoshimitsu K, Irie H et al (2003) Fitz-Hugh–Curtis syndrome. J Comput Assist Tomogr 27:786–791
31. Tsujikawa T, Tsuchida T, Yoshida Y et al (2011) Role of PET/CT in gynecological tumors based on the revised FIGO staging classification. Clin Nucl Med 36:114–118
32. Hashefi M, Curiel R (2011) Future and upcoming non-neoplastic applications of PET/CT imaging. Ann N Y Acad Sci 1228:167–174
33. Henriksen G, Herz M, Hauser A et al (2004) Synthesis and preclinical evaluation of the choline transport tracer deshydroxy-[18F]fluorocholine ([18F]dOC). Nucl Med Biol 31:851–858